Reaction Mechanism of the Selective Reduction of CO_2 to CO by a Tetraaza $[Co^{II}N_4H]^{2+}$ Complex in the Presence of Protons

Journal:	*Physical Chemistry Chemical Physics*
Manuscript ID	CP-ART-03-2018-001963.R2
Article Type:	Paper
Date Submitted by the Author:	01-Sep-2018

Complete List of Authors:	Garza, Alejandro; University of California - Berkeley, Chemistry PAKHIRA, SRIMANTA; Florida State University, Department of Chemical Engineering; National High Magnetic Field Laboratory (NHMFL), Condensed Matter Theory Bell, Alexis; University of California, Department of Chemical and Biomolecular Engineering Mendoza-Cortes, Jose ; Florida State University, Department of Chemical Engineering; Florida A&M University-Florida State University College of Engineering, Head-Gordon, Martin; University of California - Berkeley, Chemistry

Journal Name

ARTICLE TYPE

Cite this: DOI: 10.1039/xxxxxxxxxx

Reaction Mechanism of the Selective Reduction of CO_2 to CO by a Tetraaza $[Co^{II}N_4H]^{2+}$ Complex in the Presence of Protons

Alejandro J. Garza,[a] Srimanta Pakhira,[b,c] Alexis T. Bell,[a,d] , Jose L. Mendoza-Cortes,[a,b,c] and Martin Head-Gordon[a,e]

Received Date
Accepted Date

DOI: 10.1039/xxxxxxxxxx

www.rsc.org/journalname

The tetraaza $[Co^{II}N_4H]^{2+}$ complex (**1**) is remarkable for its ability to selectively reduce CO_2 to CO with 45% Faradaic efficiency and a CO to H_2 ratio of 3:2. We employ density functional theory (DFT) to determine the reasons behind the unusual catalytic properties of **1** and the most likely mechanism for CO_2 reduction. The selectivity for CO_2 over proton reduction is explained by analyzing the catalyst's affinity for the possible ligands present under typical reaction conditions: acetonitrile, water, CO_2, and bicarbonate. After reduction of the catalyst by two electrons, formation of $[Co^{I}N_4H]^{+}-CO_2^{-}$ is strongly favored. Based on thermodynamic and kinetic data, we establish that the only likely route for producing CO from here consists of a protonation step to yield $[Co^{I}N_4H]^{+}-CO_2H$, followed by reaction with CO_2 to form $[Co^{II}N_4H]^{2+}-CO$ and bicarbonate. This conclusion corroborates the idea of a direct role of CO_2 as a Lewis acid to assist in C−O bond dissociation, a conjecture put forward by other authors to explain recent experimental observations. The pathway to formic acid is predicted to be forbidden by high activation barriers, in accordance with the products that are known to be generated by **1**. Calculated physical observables such as standard reduction potentials and the turnover frequency for our proposed catalytic cycle are in agreement with available experimental data reported in the literature. The mechanism also makes a prediction that may be experimentally verified: that the rate of CO formation should increase linearly with the partial pressure of CO_2.

1 Introduction

Transition metals supported by tetradentate, redox-non-innocent ligand macrocycles are well known for reducing protons to dihydrogen [1–8]. However, some are also capable of reducing CO_2 to CO, formate, and oxalate [9–15]. This offers the intriguing possibility of utilizing CO_2 to generate valuable chemicals or store energy from wind or solar radiation in the form of liquid fuels. Selectivity towards generating products of CO_2 reduction is one of the main limitations for practical applications of this process, although there has been steady progress in this area over the last decades.

CO_2-reducing cobalt and nickel phthalocyanines were first reported by Meshitsuka *et al.* in 1974 [9]. Since then, a wide-range of catalysts based on different host ligands have been reported; e.g., cyclam [16–18], phthalocyanines [19–21], porphyrins [22–24], and polypyridines [25–27], to name a few. More recently, it has been demonstrated that tetraaza macrocyclic complexes of late first row transition metals, such as $[Co^{II}$-$N_4H(MeCN)]^{2+}[B(C_6H_5)_4^{-}]_2$ (N_4H =2,12-dimethyl-3,7,11,17-tetraazabicyclo-[11,3,1]-heptadeca-1(17),2,11,13,15-

[a] *Joint Center for Artificial Photosynthesis, Lawrence Berkeley National Laboratory, Berkeley, CA 94720, USA*
[b] *Department of Physics, Scientific Computing, Materials Science and Engineering, High Performance Material Institute, Condensed Matter Theory-National High Magnetic Field Laboratory, Florida State University, Tallahassee, FL 32310, USA*
[c] *Department of Chemical & Biomedical Engineering, Florida A&M University - Florida State University, Joint College of Engineering, Tallahassee, FL 32310, USA*
[d] *Department of Chemical and Biomolecular Engineering, University of California, Berkeley, CA 94720, USA*
[e] *Department of Chemistry, University of California, Berkeley, CA 94720, USA*
* *E-mail: mendoza@eng.famu.fsu.edu, E-mail: mhg@cchem.berkeley.edu*

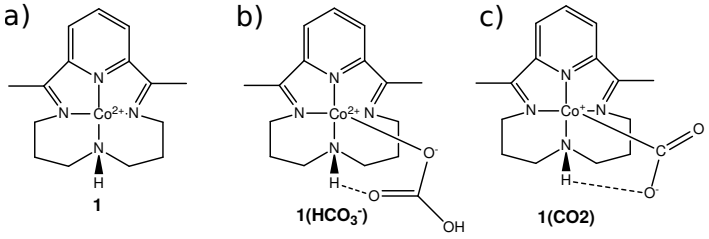

Fig. 1 Structure of (a) $[Co^{II}N_4H]^{2+}$ (**1**), (b) adduct of **1** with HCO_3^- (c) adduct of (two-electron reduced) **1** with CO_2

pentaene), are efficient catalysts for hydrogen evolution [28–30] and CO_2 reduction [31–33], either electrocatalytically, or by using a visible light sensitizer in the presence of a sacrificial electron donor. Among the tetraaza catalysts, $[Co^{II}N_4H]^{2+}$ (compound **1** in Figure 1) stands out for its ability to generate CO with 45% Faradaic efficiency and an unusual CO to H_2 ratio of 3:2 near the $Co^{I/0}$ potential [30]. This catalyst is remarkable because cobalt N_4-macrocycles are known for favoring proton reduction [34]. Furthermore, **1** is highly selective towards CO over other carbon products: no formate or oxalate are produced [30]. The cause of the atypical catalytic activity of **1** is not understood, neither is the mechanism by which **1** reduces CO_2 known, although **1(HCO$_3^-$)** and **1(CO$_2$)** (see Figure 1) have been observed by FT-IR spectroscopy [35]. The presence of **1(HCO$_3^-$)** indicates that bicarbonate may be involved in the reaction mechanism; however, this is unusual for this type of compound and has not been confirmed either experimentally or theoretically.

Herein, we employ density functional theory (DFT) to explain the selectivity of **1** towards reduction of CO_2 to CO. Our calculations corroborate the preference of **1** for binding CO_2 rather than protons, and provide insight into the structural origin of this preference. We derive the most likely mechanism for CO_2 reduction, and compute observables such as the turnover frequency (TOF) using the energetic span model. These results agree with, and explain, various notable experimental observations, including the selectivity for CO over formate. Importantly, our conclusions strongly support the hypothesis that bicarbonate plays a critical role in the reaction mechanism. This study is an extension of our previous theory-experiment work on the subject [36].

2 Theory and Computational Details

Gas phase calculations were carried out using the QChem software package [37]. Calculations in water and acetonitrile were performed with the polarizable continuum model [38] implemented in Gaussian [39] (experiments on **1** are normally carried out on wet acetonitrile, i.e. ≈ 10 M water in CH_3CN). The results that we focus the discussion on are for the acetonitrile medium, but we remark that reaction energies in water and acetonitrile do not differ significantly. Transition and ground state geometries were optimized at the BP86/6-31G(d,p) level using spin-unrestricted Kohn–Sham determinants. This level of theory was selected on the basis of good agreement with available experimental structural and spin-state data for **1**; BP86 yielded better results than PBE, B3LYP, and B97X-D (further details were presented in our previous work on ref. [36]). The results reported here are for low-spin states of the catalyst, which corresponds to the ground state according to both BP86 simulations and experimental measurements [30, 36]. Free energies were obtained by correcting electronic energies with their corresponding enthalpic and entropic contributions at 298 K using vibrational frequency data and standard formulas [40]. We noticed, however, that the ideal gas, rigid rotor and harmonic oscillator formulas significantly overestimate the entropy of CO_2 and H_2O in solution (translation and rotation motions are sharply reduced in solution [41, 42]). This results in spurious ΔG values for bimolecular reactions. Thus, we used reported experimental entropies in aqueous solution to compute the thermal corrections of these molecules ($\Delta S_{\text{sol}\longrightarrow\text{gas}} = 126.0$ and 118.9 J/mol·K for CO_2 and H_2O, respectively [43–45]).

We also encountered difficulties in calculating free energies for protonation reactions because of the poor description of the solvation energy of protons (and hydronium ions) by implicit solvent models. To circumvent this issue, we followed other authors [46] and employed accurate proton solvation energies from high-level *ab initio* calculations (-260.2 kcal/mol for acetonitrile [47]) which agree, within experimental error, with experimental values.

Turnover frequencies (TOFs) for the possible catalytic cycles were estimated with the energetic span model [48–50]:

$$\text{TOF} = \frac{kT}{h} \cdot \frac{e^{-\Delta G_r/kT} - 1}{\sum_{i,j} e^{(T_i - I_j - \delta G_{ij})/kT}} \tag{1}$$

$$\delta G_{ij} = \begin{cases} \Delta G_r, & \text{if } i > j \\ 0, & \text{if } i \leq j, \end{cases}$$

where ΔG_r is the total reaction free energy, and T_j and I_j are the free energies of the jth transition state and intermediate in the cycle, respectively.

3 Results and Discussion

3.1 Binding to water, bicarbonate, and carbon dioxide

Table 1 lists the acetonitrile-medium free energies for binding **1** to species that would normally be found in the reaction: acetonitrile, water, bicarbonate, and carbon dioxide. Three oxidation states of **1** are considered; reduction potentials *vs* the standard hydrogen electrode (SHE) are also reported (the absolute SHE potential is taken as 4.43 V [51]). In its highest oxidation state, $[Co^{II}N_4H]^{2+}$ is unable to bind CO_2 ($\Delta G_{\text{bind}} = 2.9$ kcal/mol), and instead binds

Table 1 Calculated standard reduction potentials (*vs* the SHE) and free energies of binding (in acetonitrile) for complexes of **1** with bicarbonate, acetonitrile, water, and carbon dioxide in different oxidation states.

	Ligand (E°/V)				
Species	None	HCO_3^-	MeCN	H_2O	CO_2
$[Co^{II}N_4H]^{2+}$	+0.08	−0.71	−0.22	+0.07	+0.47
$[Co^{I}N_4H]^{+}$	−1.33	−1.69	−1.42	−1.32	−1.01
	ΔG_{bind}/kcal·mol^{-1}				
$[Co^{II}N_4H]^{2+}$		−28.7	−7.7	−9.8	+2.9
$[Co^{I}N_4H]^{+}$		−10.3	+0.9	−6.2	−6.1
$[Co^{0}N_4H]$		−1.9	+4.1	−6.4	−13.3

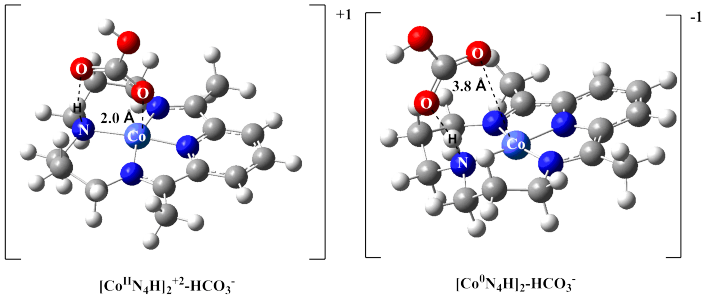

Fig. 2 Optimized structures of the adducts of bicarbonate with the doubly-charged and neutral catalyst.

preferentially to bicarbonate ($\Delta G_{bind} = -28.7$ kcal/mol). Positive charge on the metal center and a favorable O···HN hydrogen bond (see Fig. 1b) are responsible for the strong interaction between HCO_3^- and **1**; the Mulliken charge on Co reduces from 1.12 to 0.97 upon complexation and the Co-O distance is only 2.0 Å (see Fig. 2). The hydrogen bond between one of the oxygen atoms in bicarbonate and the NH group in **1** has been observed experimentally by infrared spectroscopy [35], and is present in the BP86-optimized geometry; the length and angle of the H-bond are 1.703 Å and 163.6° (Fig. 2), respectively, indicating a strong interaction. Consistent with these results, **1(HCO$_3^-$)** has been experimentally determined to be the dominant species for the oxidized catalyst in the presence of CO_2 in wet acetonitrile [35]. The calculated $E^\circ = -0.22$ V for the $[Co^{II}N_4H]^{2+}$–MeCN complex is very close to the measured reduction potential potential of $[Co^{II}N_4H]^{2+}$ in acetonitrile [30] ($E^\circ = -0.28$ V).

Upon reduction of the catalyst by one electron, CO_2 is calculated to have substantial binding with the catalyst ($\Delta G_{bind} = -6.1$ kcal/mol), but HCO_3^- is still largely the preferred ligand ($\Delta G_{bind} = -10.3$ kcal/mol). The affinity for H_2O is anticipated to be similar to that for CO_2 ($\Delta G_{bind} = -6.2$ kcal/mol). These findings are in accordance with the spectroscopic measurements in ref. [52], which detected $[Co^{II}N_4H]^{2+}$–HCO_3^-, $[Co^{I}N_4H]^{+}$–HCO_3^-, and $[Co^{I}N_4H]^{+}$–CO_2, but not $[Co^{II}N_4H]^{2+}$–CO_2. However, the $[Co^{II}N_4H]^{2+}$–H_2O cannot be deconvoluted in the FT-IR measurments as it is covered under the large bulk water signal. The calculated standard reduction potential of $[Co^{I}N_4H]^{+}$ ($E^\circ = -1.33$ V *vs* the SHE) is also in agreement with the reported experimental value ($E^\circ = -1.24$ V) in MeCN [30]. The $E^\circ = -1.42$ V for $[Co^{I}N_4H]^{+}$–MeCN is also reasonably close to experiment.

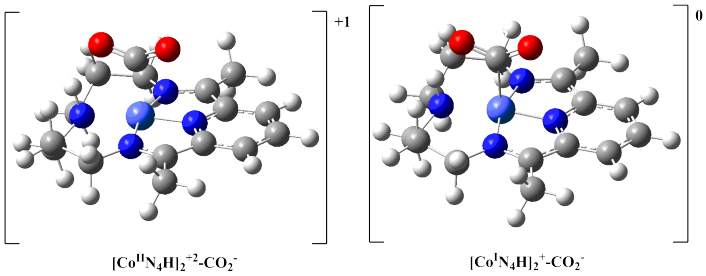

Fig. 3 Optimized structures of the adducts of CO_2 with the singly-charged and neutral catalyst.

It is not until **1** is reduced by a second electron that CO_2 binding ($\Delta G_{bind} = -13.3$ kcal/mol) becomes dominant over binding to water (−6.4 kcal/mol) and bicarbonate (−1.9 kcal/mol). The loss of charge at the metal center greatly weakens its interaction with the O atom of bicarbonate, increasing the Co-O distance from 2.0 to 3.8 Å (Fig. 2). The doubly-reduced $[Co^{0}N_4H]$ is known to be the catalytically active species: reduction products are not observed unless a sensitizer with enough reduction potential to generate $[Co^{0}N_4H]$ is present [35, 36]. Hence, the unusual selectivity of **1** for CO_2 reduction can be traced to the greater affinity of $[Co^{0}N_4H]$ for CO_2 over water. This enhanced CO_2 affinity can in turn be attributed to two factors: one electronic and one structural. The first one is related to a charge transfer from the catalyst to CO_2: when bound to the doubly reduced neutral catalyst, CO_2 becomes partially negative (resulting in a bent structure with a bond angle of 132.0° as shown in Fig. 2), whilst the catalyst acquires a partial positive charge localized at the transition metal center. This picture is corroborated by the the sum of the Mulliken charges in the oxygen atoms of CO_2 (−1.0), and the charges on cobalt (0.66), and the carbon atom of CO_2 (0.39). The structural factor is a hydrogen bond between a CO_2 oxygen atom and the NH group in the tetraaza ring; the length and angle of this H-bond are 1.797 Å and 139.6°, respectively. In comparison, the length of this same H-bond is 1.911 Å in the singly reduced $[Co^{I}N_4H]^{+}$–CO_2 complex. Thus, the (Lewis) acid-base properties of the catalyst synergize with its structure to boost CO_2 affinity by transferring negative charge to the latter and, consequently, strengthening the O···HN bond. Note that although intramolecular H-bonds are rare in protic solvents [53, 54], they can be quite favorable in aprotic solvents and, in fact, signals corresponding to a CO_2···HN H-bond are present in the IR spectra of the reduced catalyst in acetonitrile [35]. *A harmonic vibrational analysis has been carried out on the equilibrium structures using the same DFT*

Table 2 Comparison of experimentally available [35] signature vibrational frequencies (in cm^{-1}) with data calculated in this work.

Species	Mode	$\tilde{\nu}_{calc.}$	$\tilde{\nu}_{expt.}$
$[Co^{II}N_4H]^{2+}$	NH stretch	3321	3237
$[Co^{I}N_4H]^{+}$	NH stretch	3307	3251
$[Co^{II}N_4H]^{2+}$–$HCO3^{-}$	CO asymm. stretch	1621	1674
	CO symm. stretch	1372	1640
	NH stretch	2833	3217
$[Co^{II}N_4H]^{2+}$–$CO2^{-}$	CO asymm. stretch	1842	1656
	CO symm. stretch	1249	1347
	NH stretch	3245	3230
$[Co^{I}N_4H]^{+}$–$CO2^{-}$	CO asymm. stretch	1711	1635
	CO symm. stretch	1355	1356
	NH stretch	3092	NA

method, and the frequencies are tabulated in Table 2 along with the experimental data wherever available. Computed signature IR frequencies are compared with the available experimental data [35] in Table 2. *The present DFT computations show that the calculated frequencies are well harmonized with the experiments within about 100 cm^{-1}. Some cases, the DFT results overestimated the experimental results.* The experimental redshift in the NH stretch signal attributed to $CO_2\cdots$HN H-bonding is clearly present in the DFT predictions. However, the calculated NH red shift is exaggerated as compared to experiment. This is most likely due to the lack of specific solvent-solute interactions in the PCM, which would weaken the intramolecular hydrogen bond. Still, the agreement seems reasonable considering the level of theory, the use of an implicit solvation model, and the fact that counterion effects are not included.

3.2 Mechanism of CO_2 reduction

The most likely mechanism of CO_2 reduction is shown in Fig. 4. The catalyst remains preferentially bound to HCO_3^- in the +2 and +1 oxidation states. Complexation with bicarbonate lowers the reduction potential of of the catalyst by −0.79 and −0.36 V for the first and second electron additions, respectively. However, as noted above, CO_2 binding is thermodynamically favored over HCO_3^- binding for the doubly-reduced, neutral catalyst by 11.4 kcal/mol. As detailed below and corroborating experimental observations, we find that the complex that can roughly be described as $[Co^{I}N_4H]^{+}$–CO_2^- (**5** in Fig. 4; see also Fig. 3) is the key intermediate leading to CO.

In our derivation of the mechanism below, we assume that protons are available to facilitate reactions. This assumption is reasonable because spectroscopic measurements [35] and our own calculations in Table 1 indicate that, in a saturated CO_2 solution, the oxidized catalyst exists predominantly as **1(HCO$_3^-$)**. The bicarbonate ligand is generated from CO_2 and H_2O, resulting in protons being available in the wet acetonitrile medium. Following other authors [46], the total free energy of a proton in solution is determined from high-level *ab initio* calculations [47] and utilized to compute free energy differences (see Theory and Computational Details).

After formation of $[Co^{I}N_4H]^{+}$–CO_2^-, the most favorable elementary step that we have identified is protonation of the CO_2 oxygen atom:

$$[Co^{I}N_4H]^{+}-CO_2^- + H^+ \longrightarrow [Co^{I}N_4H]^{+}-CO_2H. \qquad (2)$$

This is a fast and highly exergonic process with a calculated $\Delta G^{\ddagger} = 5.0$ kcal/mol and a $\Delta G = -20.6$ kcal/mol. Alternative reactions such as protonation on the C atom

$$[Co^{I}N_4H]^{+}-CO_2^- + H^+ \longrightarrow [Co^{I}N_4H]^{+}-HCO_2 \qquad (3)$$

or reaction with CO_2 to form CO_3^{2-} and CO

$$[Co^{I}N_4H]^{+}-CO_2^- + CO_2 \longrightarrow [Co^{II}N_4H]^{2+}-CO + CO_3^{2-} \qquad (4)$$

do not appear to be competitive. The reaction in eq. 3 would (most likely) lead to formate, which is not produced by catalyst **1**. Not only this, but protonation on the carbon atom is chemically counterintuitive given that the negative charge is localized in the O atoms. Consistent with this notion, the free energy barrier for this reaction is estimated to be much higher (≈ 32 kcal/mol; *vide infra*) than the 5 kcal/mol for oxygen protonation. Likewise, the $\Delta G^{\ddagger}$ to generate CO and carbonate ion (eq. 4) is predicted to be about 40 kcal/mol. This explains the experimental observation of CO_2 reduction not taking place in the absence of water [36]: protons coming from the reaction of CO_2 with water are required for eq. 2 to occur and eventually lead to CO, as the proton-free eq. 4 is not a viable path. In $[Co^{I}N_4H]^{+}-CO_2^-$, the C−O bond has double bond character: the length of the C−O bond for the oxygen forming the H-bond with the NH group is 1.265 Å, whereas the length of the other C−O bond is 1.240 Å. This is, presumably, the reason for the high $\Delta G^{\ddagger}$ required to break one of these bonds via eq. 4.

After the initial protonation, eq. 2, the lowest energy path consists of the CO_2H group reacting with CO_2 to form bicarbonate and CO:

$$[Co^{I}N_4H]^{+}-CO_2H + CO_2 \longrightarrow [Co^{II}N_4H]^{2+}-CO + HCO_3^-. \qquad (5)$$

The structure of the transition state for this reaction is shown in Fig. 5. With a calculated $\Delta G^{\ddagger} = 20.1$ kcal/mol, this is the rate-determining step of the catalytic cycle. Nonetheless, the activation free energies for other possible reactions are much higher in our simulations (see discussion below and SI). The barrier for a second protonation on an oxygen atom to form CO and water

$$[Co^{I}N_4H]^{+}-CO_2H + H^+ \longrightarrow [Co^{II}N_4H]^{2+}-CO + H_2O \qquad (6)$$

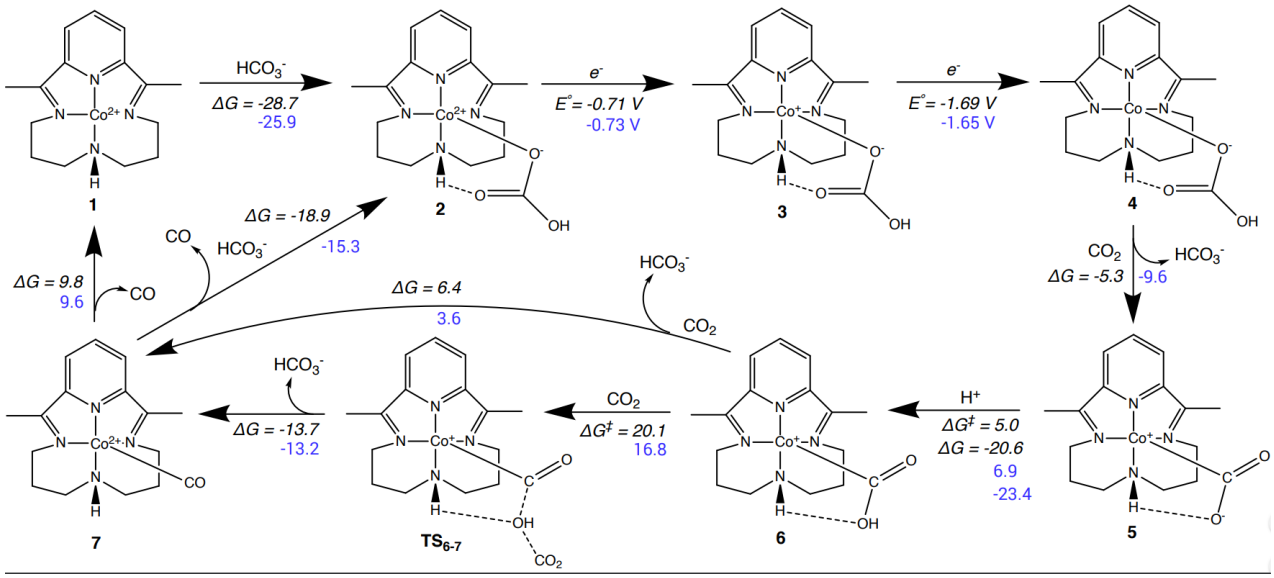

Fig. 4 Proposed mechanism for the CO_2 reduction catalytic cycle. Free energies are in kcal/mol with values in black and blue indicating that the calculations are in acetonitrile and water, respectively.

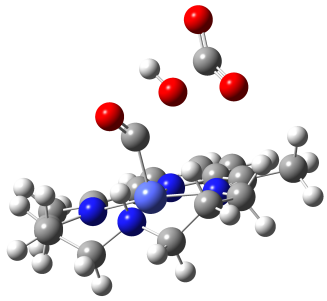

Fig. 5 Optimized structure of the transition state of the rate-determining step of the reaction (**TS**$_{6-7}$), which leads to CO and regenerationg of bicarbonate.

was computed as $\Delta G^{\ddagger} = 61.6$ kcal/mol. It is not immediately clear why the barrier to form water is so high as compared to that for forming bicarbonate; we verified various possible ways in which the proton could attack CO_2H but did not find lower activation energies. We conclude that the CO_2H group attached to the catalyst is an acid, not a base, and, in a certain way, behaves similarly to bicarbonate or carbonic acid. An additional factor contributing to the HCO_3^- preference is the electrostatic interaction between the positively-charged catalyst and the negatively-charged bicarbonate. As reflected on Table 1, the interaction of HCO_3^- with the doubly charged catalyst is about 20 kcal/mol stronger than the interaction of the latter with water.

Two closely related steps that can occur are protonation of the OH end of CO_2H without simultaneous C−O bond cleavage

$$[Co^{I}N_4H]^+ - CO_2H + H^+ \longrightarrow [Co^{I}N_4H]^+ - CO_2H_2^+, \qquad (7)$$

and reaction of $[Co^{I}N_4H]^+ - CO_2H$ with water to form CO, OH^-, and water

$$[Co^{I}N_4H]^+ - CO_2H + H_2O \longrightarrow [Co^{II}N_4H]^{2+} - CO + OH^- + H_2O. \qquad (8)$$

However, the structure of $[Co^{I}N_4H]^+ - CO_2H_2^+$ does not appear to be stable; we were unable to optimize a geometry for this complex that did not revert to $[Co^{II}N_4H]^{2+} - CO$ and water. Eq. 8 is analogous to eq. 6, except that water, instead of a proton, is acting as a Brønsted acid. This would increase $\Delta G^{\ddagger}$ compared to the already too-high $\Delta G^{\ddagger}$ of eq. 6. Therefore we do not consider the reaction in eq. 8 a possibility.

Another plausible reaction that $[Co^{I}N_4H]^+ - CO_2H$ could undergo consists of a proton attack on the C atom to yield formic acid:

$$[Co^{I}N_4H]^+ - CO_2H + H^+ \longrightarrow [Co^{II}N_4H]^{2+} + HCO_2H. \qquad (9)$$

The BP86 functional gives a $\Delta G^{\ddagger} = 31.8$ kcal/mol for this process. This is again in agreement with chemical intuition as the C atom has a partial positive charge (Mulliken charge = 0.35), and one would expect it to be less basic than the O atoms. But there seem to be further reasons related to the catalyst's structure that are responsible for the selectivity towards CO as a product. When we optimize the structure of the transition state, the proton is first captured by the negatively-charged N atoms of the tetraaza

ring, before being transferred to the carbon atom. This appears to be a result of the orientation of the CO_2H group, which is anchored by the $CO_2H\cdots HN$ hydrogen bond. The basic N atoms in the catalyst do not capture the proton if we allow for the latter to attack from above (rather than from a side/below); however, this results in an even larger barrier ($\Delta G^{\ddagger} = 60.6$ kcal/mol) because the density that the C atom can donate is located around the C−Co bond. Thus, because of H-bonding, the position of the catalyst's NH group is crucial in determining not only the affinity for CO_2 binding, but also the selectivity for CO by preventing a direct proton attack on the C atom to generate formic acid. The fact that the carbon atom does not interact favorably with protons is in line with the aforementioned proposition that the chemistry of the CO_2H group attached to the catalyst is akin to that of carbonic acid or the bicarbonate ion.

Yet another possibility is the protonation of a second oxygen atom in CO_2H:

$$[Co^{I}N_4H]^{+}-CO_2H + H^{+} \longrightarrow [Co^{I}N_4H]^{+}-[C(OH)_2]^{+}. \qquad (10)$$

Eq. 10 is unlikely to occur as its $\Delta G^{\ddagger}$ is about 30 kcal/mol higher than the $\Delta G^{\ddagger}$ for CO and bicarbonate production according to eq. 5. The reaction ΔG for eq. 10 is also substantially endergonic (11.1 kcal/mol). The high relative energy of $[Co^{I}N_4H]^{+}-[C(OH)_2]^{+}$ is unsurprising given that it places further positive charge on the C atom that is linked to Co^{+} center (chemical intuition is, once more, spot-on).

Not only is the mechanism on Fig. 4 predicted to be the main route for CO_2 reduction, but the TOF computed for this mechanism is also in agreement with experimental data. Using the energetic span model (eq. 1), we calculate a TOF = 1×10^{-2} s^{-1}. From experimental data, the TOF for catalyst **1** is about 1×10^{-3} s^{-1} [30]. In the energy representation, these rates correspond to effective free energies of activation of 20.1 and 21.4 kcal/mol for the calculated and experimental rates, respectively. Hence, the reaction pathway on Fig. 4—the only pathway in which bicarbonate plays a central role—is the only one compatible with experimental observations, according to our calculations.

As noted earlier, recent experimental studies of catalyst **1** have pointed to bicarbonate as an important player in the catalytic cycle [35]. A direct role of CO_2 as a Lewis acid to assist C−O bond dissociation has also been suggested to explain observations related to the activity of a Ni-cyclam catalyst [55]. However, to the best of our knowledge, all experimental observations related to the role of CO_2/HCO_3^- are inconclusive. We are not aware of other theoretical studies considering this possibility, but our results certainly support the ideas put forward in these experimental studies. Based on our calculated $\Delta G^{\ddagger}$ values for the possible paths to CO, CO_2 reduction to CO would not occur if it was not for CO_2 itself acting as a Lewis acid to facilitate C−O bond breaking and form HCO_3^-. Notice also that bicarbonate plays an additional role by binding to the oxidized catalyst and displacing CO. Otherwise, CO could poison the catalyst ($\Delta G_{\text{bind}} = -9.8$ kcal/mol). It is worth noting that a recent (experimental) study has highlighted the importance of bicarbonate in the reduction of CO_2 to CO on metallic gold surfaces [56]. This work also demonstrated that the equilibrium reaction

$$^{13}CO_{2\,(aq)} + H\,^{12}CO_3^- \longleftrightarrow {}^{12}CO_{2\,(aq)} + H\,^{13}CO_3^- \qquad (11)$$

is fast on the timescale of the CO_2 reduction reaction (sufficiently fast that it alters the isotopic composition of $CO_{2\,(aq)}$ and $CO_{2\,(gas)}$ in a different manner). This observation provides further support for our mechanism, along with the idea that CO_2H behaves like HCO_3^- or H_2CO_3 when attached to the catalyst.

Lastly, we remark that our proposed mechanism gives a prediction regarding the kinetics of the reaction that may be verified experimentally. Assuming that the catalyst-CO_2 complex exists mostly as $[Co^{I}N_4H]^{+}-CO_2H$ (**6**) under reaction conditions, the rate of CO formation should increase linearly with the partial pressure of CO_2. To the best of our knowledge, the dependence of the rate of the reaction on the partial pressure of CO_2 has not been reported in the literature. Thus, we suggest that investigating this dependence is a well grounded way to probe the mechanism of CO_2 reduction catalyzed by **1**.

4 Conclusions

Based on DFT calculations, we deduced a mechanism for the selective reduction of CO_2 to CO by the tetraaza $[Co^{II}N_4H]^{2+}$ catalyst (**1**). Our simulations provide structural insight on the reasons for the catalyst's selectivity: hydrogen bonding between bound CO_2 and the NH group in the tetraaza ring is vital. Analysis of our results confirms previous speculation (from experimental observations) regarding the role of CO_2 acting as a Lewis acid to assist in the dissociation of the C−O bond to generate HCO_3^- and CO. This step is rate-determining and the calculated TOF of 1×10^{-3} s^{-1} is in agreement with the experimental value of 1^{-2} s^{-1} (in terms of energy, less than 2 kcal/mol difference in effective $\Delta G^{\ddagger}$ for the catalytic cycle). No other CO_2 reduction reaction pathway was found to be competitive: the activation energies for alternative paths are higher than the "$CO + HCO_3^-$" path by a large (> 10 kcal/mol) margin—much larger than the typical DFT error range (≈ 4 kcal/mol). Considering this in tandem with the aforementioned experimental reports from the literature, does not leave much room for other possible CO_2 reduction pathways. Finally, the mechanism makes a prediction that may be experimentally verified: that the rate of CO formation should increase linearly with the partial pressure of CO_2.

5 Acknowledgements

A.J.G, A.T.B., and M.H.G acknowlege the Joint Center for Artificial Photosynthesis, a DOE Energy Innovation Hub, supported

through the Office of Science of the U.S. Department of Energy under Award DE-SC00004993. S.P. and J.L.M-C. were supported by Florida State University (FSU). The computing work perfomed at LBNL used resources of the National Energy Research Scientific Computing Center, a DOE Office of Science User Facility supported by the Office of Science of the U.S. Department of Energy under Contract No. DE-AC02-05CH11231; the computing work at FSU was performed on the High Performance Computer cluster at the FSU Research Computing Center.

References

1 J. L. Dempsey, B. S. Brunschwig, J. R. Winkler, and H. B. Gray, *Accounts of Chemical Research*, 2009, **42**(12), 1995–2004.

2 X. Hu, B. S. Brunschwig, and J. C. Peters, *Journal of the American Chemical Society*, 2007, **129**(29), 8988–8998.

3 S. Varma, C. E. Castillo, T. Stoll, J. Fortage, A. G. Blackman, F. Molton, A. Deronzier, and M.-N. Collomb, *Physical Chemistry Chemical Physics*, 2013, **15**(40), 17544–17552.

4 C. C. McCrory, C. Uyeda, and J. C. Peters, *Journal of the American Chemical Society*, 2012, **134**(6).

5 C.-F. Leung, Y.-Z. Chen, H.-Q. Yu, S.-M. Yiu, C.-C. Ko, and T.-C. Lau, *International Journal of Hydrogen Energy*, 2011, **36**(18), 11640–11645.

6 D. Z. Zee, T. Chantarojsiri, J. R. Long, and C. J. Chang, *Accounts of chemical research*, 2015, **48**(7), 2027–2036.

7 N. Kaeffer, M. Chavarot-Kerlidou, and V. Artero, *Accounts of chemical research*, 2015, **48**(5), 1286.

8 E. M. Nichols, J. S. Derrick, S. K. Nistanaki, P. T. Smith, and C. J. Chang, *Chemical Science*, 2018.

9 S. Meshitsuka, M. Ichikawa, and K. Tamaru, *Journal of the Chemical Society, Chemical Communications*, 1974, (5), 158–159.

10 W.-H. Wang, Y. Himeda, J. T. Muckerman, G. F. Manbeck, and E. Fujita, *Chem. Rev.*, 2015, **115**(23), 12936–12973.

11 C. Finn, S. Schnittger, L. J. Yellowlees, and J. B. Love, *Chemical Communications*, 2012, **48**(10), 1392–1399.

12 J. Schneider, H. Jia, J. T. Muckerman, and E. Fujita, *Chemical Society Reviews*, 2012, **41**(6), 2036–2051.

13 M. Rudolph, S. Dautz, and E.-G. Jäger, *Journal of the American Chemical Society*, 2000, **122**(44), 10821–10830.

14 R. Angamuthu, P. Byers, M. Lutz, A. L. Spek, and E. Bouwman, *Science*, 2010, **327**(5963), 313–315.

15 A. Tinnemans, T. Koster, D. Thewissen, and A. Mackor, *Recueil des Travaux Chimiques des Pays-Bas*, 1984, **103**(10), 288–295.

16 M. Beley, J.-P. Collin, R. Ruppert, and J.-P. Sauvage, 1984, (19), 1315–1316.

17 M. Beley, J. P. Collin, R. Ruppert, and J. P. Sauvage, *J. Am. Chem. Soc.*, 1986, **108**(24), 7461–7467.

18 J. D. Froehlich and C. P. Kubiak, *Inorganic chemistry*, 2012, **51**(7), 3932–3934.

19 T. Yoshida, K. Kamato, M. Tsukamoto, T. Iida, D. Schlettwein, D. Wöhrle, and M. Kaneko, *Journal of Electroanalytical Chemistry*, 1995, **385**(2), 209–225.

20 T. Abe, T. Yoshida, S. Tokita, F. Taguchi, H. Imaya, and M. Kaneko, *Journal of Electroanalytical Chemistry*, 1996, **412**(1-2), 125–132.

21 J. Grodkowski, T. Dhanasekaran, P. Neta, P. Hambright, B. S. Brunschwig, K. Shinozaki, and E. Fujita, *The Journal of Physical Chemistry A*, 2000, **104**(48), 11332–11339.

22 M. Hammouche, D. Lexa, M. Momenteau, and J. M. Saveant, *Journal of the American Chemical Society*, 1991, **113**(22), 8455–8466.

23 D. Behar, T. Dhanasekaran, P. Neta, C. Hosten, D. Ejeh, P. Hambright, and E. Fujita, *The Journal of Physical Chemistry A*, 1998, **102**(17), 2870–2877.

24 S. Lin, C. S. Diercks, Y.-B. Zhang, N. Kornienko, E. M. Nichols, Y. Zhao, A. R. Paris, D. Kim, P. Yang, O. M. Yaghi, et al., *Science*, 2015, **349**(6253), 1208–1213.

25 J. Hawecker, J.-M. Lehn, and R. Ziessel, *Journal of the Chemical Society, Chemical Communications*, 1984, (6), 328–330.

26 B. Gholamkhass, H. Mametsuka, K. Koike, T. Tanabe, M. Furue, and O. Ishitani, *Inorganic chemistry*, 2005, **44**(7), 2326–2336.

27 M. Bourrez, F. Molton, S. Chardon-Noblat, and A. Deronzier, *Angewandte Chemie*, 2011, **123**(42), 10077–10080.

28 C. Arana, S. Yan, M. Keshavarz-K., K. T. Potts, and H. D. Abruna, *Inorg. Chem.*, 1992, **31**(17), 3680–3682.

29 S. Sakaki and Y. Musashi in *Computational Modeling of Homogeneous Catalysis*, ed. F. Maseras and A. Lleds, number 25 in Catalysis by Metal Complexes; Springer US, 2002; pp. 79–105.

30 D. C. Lacy, C. C. McCrory, and J. C. Peters, *Inorganic chemistry*, 2014, **53**(10), 4980.

31 T. Ogata, S. Yanagida, B. S. Brunschwig, and E. Fujita, *J. Am. Chem. Soc.*, 1995, **117**(25), 6708–6716.

32 C. Costentin, M. Robert, J.-M. Savant, and A. Tatin, *PNAS*, 2015, **112**(22), 6882–6886.

33 C. Federsel, A. Boddien, R. Jackstell, R. Jennerjahn, P. J. Dyson, R. Scopelliti, G. Laurenczy, and M. Beller, *Angew. Chem. Int. Ed.*, 2010, **49**(50), 9777–9780.

34 J. R. McKone, S. C. Marinescu, B. S. Brunschwig, J. R. Winkler, and H. B. Gray, *Chemical Science*, 2014, **5**(3), 865–878.

35 H. Sheng and H. Frei, *J. Am. Chem. Soc.*, 2016, **138**(31), 9959–9967.

36 M. Zhang, M. El-Roz, H. Frei, J. Mendoza-Cortes, M. Head-Gordon, D. C. Lacy, and J. C. Peters, *Journal of Physical Chemistry C*, 2015, **119**(9), 4645–4654.

37 Y. Shao, Z. Gan, E. Epifanovsky, A. T. B. Gilbert, M. Wor-

mit, J. Kussmann, A. W. Lange, A. Behn, J. Deng, X. Feng, D. Ghosh, M. Goldey, P. R. Horn, L. D. Jacobson, I. Kaliman, R. Z. Khaliullin, T. Kús, A. Landau, J. Liu, E. I. Proynov, Y. M. Rhee, R. M. Richard, M. A. Rohrdanz, R. P. Steele, E. J. Sundstrom, H. L. Woodcock III, P. M. Zimmerman, D. Zuev, B. Albrecht, E. Alguire, B. Austin, G. J. O. Beran, Y. A. Bernard, E. Berquist, K. Brandhorst, K. B. Bravaya, S. T. Brown, D. Casanova, C.-M. Chang, Y. Chen, S. H. Chien, K. D. Closser, D. L. Crittenden, M. Diedenhofen, R. A. DiStasio Jr., H. Dop, A. D. Dutoi, R. G. Edgar, S. Fatehi, L. Fusti-Molnar, A. Ghysels, A. Golubeva-Zadorozhnaya, J. Gomes, M. W. D. Hanson-Heine, P. H. P. Harbach, A. W. Hauser, E. G. Hohenstein, Z. C. Holden, T.-C. Jagau, H. Ji, B. Kaduk, K. Khistyaev, J. Kim, J. Kim, R. A. King, P. Klunzinger, D. Kosenkov, T. Kowalczyk, C. M. Krauter, K. U. Lao, A. Laurent, K. V. Lawler, S. V. Levchenko, C. Y. Lin, F. Liu, E. Livshits, R. C. Lochan, A. Luenser, P. Manohar, S. F. Manzer, S.-P. Mao, N. Mardirossian, A. V. Marenich, S. A. Maurer, N. J. Mayhall, C. M. Oana, R. Olivares-Amaya, D. P. O'Neill, J. A. Parkhill, T. M. Perrine, R. Peverati, P. A. Pieniazek, A. Prociuk, D. R. Rehn, E. Rosta, N. J. Russ, N. Sergueev, S. M. Sharada, S. Sharmaa, D. W. Small, A. Sodt, T. Stein, D. Stück, Y.-C. Su, A. J. W. Thom, T. Tsuchimochi, L. Vogt, O. Vydrov, T. Wang, M. A. Watson, J. Wenzel, A. White, C. F. Williams, V. Vanovschi, S. Yeganeh, S. R. Yost, Z.-Q. You, I. Y. Zhang, X. Zhang, Y. Zhou, B. R. Brooks, G. K. L. Chan, D. M. Chipman, C. J. Cramer, W. A. Goddard III, M. S. Gordon, W. J. Hehre, A. Klamt, H. F. Schaefer III, M. W. Schmidt, C. D. Sherrill, D. G. Truhlar, A. Warshel, X. Xua, A. Aspuru-Guzik, R. Baer, A. T. Bell, N. A. Besley, J.-D. Chai, A. Dreuw, B. D. Dunietz, T. R. Furlani, S. R. Gwaltney, C.-P. Hsu, Y. Jung, J. Kong, D. S. Lambrecht, W. Liang, C. Ochsenfeld, V. A. Rassolov, L. V. Slipchenko, J. E. Subotnik, T. Van Voorhis, J. M. Herbert, A. I. Krylov, P. M. W. Gill, and M. Head-Gordon, *Mol. Phys.*, 2015, **113**, 184–215.

38 J. Tomasi, B. Mennucci, and R. Cammi, *Chem. Rev*, 2005, **105**(8), 2999–3094.

39 M. J. Frisch, G. W. Trucks, H. B. Schlegel, G. E. Scuseria, M. A. Robb, J. R. Cheeseman, G. Scalmani, V. Barone, G. A. Petersson, H. Nakatsuji, X. Li, M. Caricato, A. V. Marenich, J. Bloino, B. G. Janesko, R. Gomperts, B. Mennucci, H. P. Hratchian, J. V. Ortiz, A. F. Izmaylov, J. L. Sonnenberg, D. Williams-Young, F. Ding, F. Lipparini, F. Egidi, J. Goings, B. Peng, A. Petrone, T. Henderson, D. Ranasinghe, V. G. Zakrzewski, J. Gao, N. Rega, G. Zheng, W. Liang, M. Hada, M. Ehara, K. Toyota, R. Fukuda, J. Hasegawa, M. Ishida, T. Nakajima, Y. Honda, O. Kitao, H. Nakai, T. Vreven, K. Throssell, J. A. Montgomery, Jr., J. E. Peralta, F. Ogliaro, M. J. Bearpark, J. J. Heyd, E. N. Brothers, K. N. Kudin, V. N. Staroverov, T. A. Keith, R. Kobayashi, J. Normand, K. Raghavachari, A. P. Rendell, J. C. Burant, S. S. Iyengar, J. Tomasi, M. Cossi, J. M. Millam, M. Klene, C. Adamo, R. Cammi, J. W. Ochterski, R. L. Martin, K. Morokuma, O. Farkas, J. B. Foresman, and D. J. Fox, Gaussian16 Revision A.03, 2016.

40 R. Jinnouchi and A. B. Anderson, *Physical Review B*, 2008, **77**(24), 245417.

41 M. Sumimoto, N. Iwane, T. Takahama, and S. Sakaki, *Journal of the American Chemical Society*, 2004, **126**(33), 10457–10471.

42 C. T. Liu, C. I. Maxwell, D. R. Edwards, A. A. Neverov, N. J. Mosey, and R. S. Brown, *Journal of the American Chemical Society*, 2010, **132**(46), 16599–16609.

43 J. Cox, D. D. Wagman, and V. A. Medvedev, *CODATA key values for thermodynamics*, Chem/Mats-Sci/E, 1989.

44 P. Linstrom and W. Mallard, Nist standard reference database number 69; national institute of standards and technology: Gaithersburg, md, 2005.

45 F. Serpa, R. Vidal, J. Filho, C. Dariva, E. Franceschi, and A. Santos.

46 I. M. Nielsen and K. Leung, *The Journal of Physical Chemistry A*, 2010, **114**(37), 10166–10173.

47 C. P. Kelly, C. J. Cramer, and D. G. Truhlar, *The journal of physical chemistry. B*, 2007, **111**(2), 408.

48 S. Kozuch and S. Shaik, *Journal of the American Chemical Society*, 2006, **128**(10), 3355–3365.

49 S. Kozuch and S. Shaik, *The Journal of Physical Chemistry A*, 2008, **112**(26), 6032–6041.

50 S. Kozuch and J. M. Martin, *ACS Catalysis*, 2011, **1**(4), 246–253.

51 R. Jinnouchi and A. B. Anderson, *The Journal of Physical Chemistry C*, 2008, **112**(24), 8747–8750.

52 H. Sheng and H. Frei, *Journal of the American Chemical Society*, 2016, **138**(31), 9959–9967.

53 J. D. Roberts, *Accounts of chemical research*, 2006, **39**(12), 889–896.

54 A. J. Garza, M. Nag, W. R. Carroll, W. A. Goddard III, and J. D. Roberts, *Journal of the American Chemical Society*, 2012, **134**(36), 14772–14780.

55 J. D. Froehlich and C. P. Kubiak, *Journal of the American Chemical Society*, 2015, **137**(10), 3565–3573.

56 M. Dunwell, Q. Lu, J. M. Heyes, J. Rosen, J. G. Chen, Y. Yan, F. Jiao, and B. Xu, *Journal of the American Chemical Society*, 2017, **139**(10), 3774–3783.